Comparing The Catalytic Activity of Mg-BTC Metal Organic Framework and Post Synthetically Modified (TiO$_2$ @ Mg-BTC) Metal Organic Framework for Cyanosilylation of Aldehydes

S. Santhana Laxmi [1] and K. Usha Nandhini [2]*

1 Department of Chemistry, Meenakshi College for Women, Chennai 600 024, India.

2* Department of Chemistry, Queen Mary's College, Chennai 600 004, India.

*Email: kusha.chem@gmail.com

Abstract

Metal–organic frameworks (MOFs) are an emerging class of porous crystalline hybrid materials synthesised by the coordination of inorganic connectors and organic linkers, which has numerous potential applications in various fields. Here we report a comparative study on Mg-BTC MOF and TiO$_2$@Mg-BTC MOF as a heterogeneous catalyst. Mg-BTC MOF was synthesised by solvothermal method and subjected to comparative study with its post synthetically modified (PSM) counterpart to understand their catalytic behaviour for cyanosilylation of aldehydes. The synthesised Mg-BTC MOF and TiO$_2$@Mg-BTC MOF were characterised by powder XRD, BET surface area, SEM, FT-IR, TGA techniques. A detailed characterization study was performed to understand the correlation between catalytic activity and morphology of the assynthesized MOF and PSM-MOF. The catalytic activity of the hybrid materials were evaluated by GC-MS analysis. The results of the catalytic reactions revealed that post synthetically modified (TiO$_2$@Mg-BTC) MOF exhibited significantly higher catalytic activity compared to Mg-BTC MOF. The enhanced catalytic efficiency is due to the incorporation of TiO$_2$ nanoparticles, which provides active sites for catalytic reactions under heterogeneous conditions. Even after repeated recycling and reuse, the catalytic ability of the catalyst retains. The impact of TiO$_2$ on the framework shows variation in texture, surface area, thermal stability and catalytic behaviour on the MOF materials. Thus, our study emphasizes the cogency of catalytically active MOFs as a heterogeneous catalyst and demonstrates the simple and effective way for the practical synthesis of fine compounds using them.

Key words: MOFs, Post Synthetic Modification, Catalyst, Hybrid materials, Cyanosilylation of Aldehydes.

Introduction:

Metal-organic frameworks (MOFs) are crystalline materials assembled themselves by the co-ordination of ligands and metal clusters[1]. These materials have attracted tremendous scientific attention during last few decades, not only driven by their highly tuneable structures but also motivated by their potential applications in the fields such as catalysis[2], electronics, gas storage and selective separation[3,4], drug delivery[5], detoxification[6], proton conductivity[7], energy storage[8], sensing and lighting[9,10] and among various fields.

Besides these useful properties, few MOFs are hindered by the physical and their chemical constraints resulting in poor performance[1]. By changing the metal atom, ligand character, ligand functionality, and synthesis environment, several porous compounds with diverse features, properties, and applications were synthesised. The structure and subsequently the characteristics of the synthesised MOFs are largely determined by the selection of the metal and linker[11]. Because of their distinct topology and tuneable features, metal organic frameworks continue to be a fascinating subject of research[12]. The majority of metal-organic frameworks (MOFs) on the market today are made from 3d or 4f metals, although there has been a recent uptick in interest in MOFs made from light main group elements like Li, Be, B, Mg, Al, or In[13].

Researchers on alkaline earth metals are limited, notably the Mg-based MOFs, which have been relatively less explored while being regarded as equally important as those focusing on other metals due to their co-ordination behaviour [14]. Mg(II) cations have a strong tendency to co-ordinately bind water molecules, which contributes to their sensitivity to moisture and therefore their instability. It can appear that the alkaline earth metals are less intriguing due to their lack of fundamentally beneficial distinctive properties. However, the alkaline earth metals offer other benefits such as their abundancy, low cost, low weight, and lack of toxicity. Various recent studies have been reported which concerns on only alkaline earth metals and their complexes deserve to be cited here[15]. MOFs synthesised by Mg^{2+} plays an

important role in exhibiting catalytic activity, their large surface area, low framework density, and malleable shape, etc.[16]

Post-synthetic modifications (PSMs) have indeed opened up new possibilities for the application of MOFs in various fields. By performing PSM on MOFs, researchers can tailor their properties and functionalities to meet specific application requirements. To ensure successful post-synthetic modifications (PSMs), it is crucial to prevent the degradation of MOFs throughout the entire reaction and maintain their integrity. Among the various methods for PSM, modifying the linker (ligand) or modifying the metallic node are commonly preferred approaches. Additionally, the adsorption or exchange of guest species is also widely employed. To enable the introduction of desired properties and increase the stability of MOF structures, modifying the surface environment of MOFs is a viable approach. One such method is metal incorporation, also known as metal doping. Metal doping is the process of introducing a new metal ion or metal complex into a pre-existing MOF structure. This can be achieved by directly coordinating the metal at specific sites within the framework or by including metal ions into the open channels of the MOF.

Inspired by the catalytic properties of nanomaterials demonstrated in the work of Rajendran et al and Sridharan et al [17,18], our study aims to explore the introduction of TiO_2 nanoparticles through post synthetic modifications. Recent advancements in nanotechnology have led to the development of highly efficient nanomaterial based catalysts, as highlighted by Chandra kishore et al[19], paving way for our current research endeavours.

This study presents a comprehensive comparison of the catalytic activity of the synthesised Mg-BTC MOF and its post synthetically modified counterpart. Through meticulous analysis of reaction yields and catalytic efficiencies, our findings shed light on the superior performance of TiO_2 @ Mg-BTC MOF in promoting the cyanosilylation of aldehydes. This investigation not only contributes to our understanding of MOF-based catalysis but also underscores the potential of post synthetic modification.

Experimental

Materials

Magnesium (II) nitrate hexahydrate [96 %, Mg $(NO_3)_2$ $6H_2O$, Sigma Aldrich,], Benzene 1,3,5 tricarboxylic acid [BTC, Sigma Aldrich, $C_9H_6O_6$, 95%]. Deionized (DI) water, N, N-dimethylformamide $(HCON(CH_3)_2)$ and ethyl alcohol anhydrous $(C_2H_5OH$, Merck 99.9%), were utilised in the catalyst preparation as solvents. There was no additional purification of the cyanosilylation chemicals because they were all of analytical grade.

Synthesis of catalysts

Synthesis of Mg-BTC MOF catalyst

In a solvent combination of 125 ml comprising water, ethanol, and DMF in a ratio of 1:1:1, 0.5 mmol of Mg $(NO_3)_2.6H_2O$ and 1 mmol of BTC were added. A magnetic stirrer was used to agitate the liquid for two hours. Then, without stirring, the mixture was kept in a stainless-steel autoclave coated with teflon and heated to 393 K. After 48 h the autoclave was cooled to room temperature at a rate of 278 K per hour. Colourless crystals were obtained which was then collected by filtration and washed with DMF and dried at 353 K for 5 h in an oven. The yield of the as synthesized catalyst was found to be 85 % based on $Mg(NO_3)_2.6H_2O$.

Post synthetic modification of Mg-BTC catalyst

The growth of TiO_2 nanoparticles on the synthesised MOF is based on the procedure followed by Hu et al[20]. 500 mg of the synthesised MOFs were air-dried at a temperature of 150°C for at least 5 h. Then it was added to the solution of 20 ml titanium (IV) butoxide and 26 ml ethyl alcohol. After sonicating the solution for 30 minutes, it was stirred for another 30 minutes. The solution was centrifuged at 4000 rpm for 20 minutes after 12 h and then the residue was washed with ethanol. The mixture was left in air for 48 h before being poured into a 250 ml teflon container containing 170 ml deionized water. A stainless-steel autoclave was then used to subject the system to air heating at 150 °C for 10 h. A solid was recovered by centrifugation and air-dried at 80°C for 72 h after cooling to ambient temperature. The titania-modified samples were designated as TiO_2@Mg-BTC MOF.

Physicochemical properties

SEM, TGA, FT-IR, PXRD and BET surface area were all employed to characterise the porous metal organic framework. Gas chromatography (GC) was used to separate the by-products of the catalytic process, and GC-MS was used to identify the products.

The crystalline structure of the material was analysed using a Bruker D8 advance powder X-ray diffraction instrument, employing Cu – K α radiation (λ = 0.154 nm) with an operating voltage of 40 KV and a current rating of 30 mA. Diffractograms were captured over a 2θ angle range, spanning from 0 to 70, with a step size of 0.02° and a count time of 10 s. To investigate the morphological characteristics of the catalysts, nitrogen adsorption at 77 K was employed, utilizing a Quanta Chrome NOVA 1000 surface analyser. Prior to testing, the samples underwent a degassing process at 573 K for 4 h to eliminate any residual moisture or adsorbed gases. The analysis employed the BET technique to quantify nitrogen adsorption,

and the BJH technique to determine cumulative volume and pore diameter based on desorption isotherms. The FT-IR spectra of the materials were acquired by utilizing KBr pellets and a Perkin Elmer Spectrum One FT-IR spectrometer, featuring a standard resolution of 1.0 cm^{-1} and spanning the spectral range from 450 cm^{-1} to 4000 cm^{-1}. To evaluate the stability of the synthesized material, thermogravimetric analysis was performed using a TGA (Perkin Elmer) Q500 Hi-Res TGA thermal analyser.

For a detailed examination of the morphology of the synthesized MOF material, scanning electron microscopy (SEM) was employed. SEM analysis was conducted using the Supra Zeiss equipment, operating at 30 KV, and equipped with a 20 mm Oxford Energy Dispersive X-ray Spectroscopy (EDS) detector. The MOF sample was allowed to air-dry at room temperature after being deposited from an ethanol solution onto a silicon plate.

Catalytic studies

Liquid-phase cyanosilylation of aldehydes with trimethyl silyl cyanide (TMSCN) was performed. A 50 ml round bottomed flask equipped with a reflux condenser was charged with aldehyde (1 mmol), TMSCN (2 mmol), pentane solvent (15 ml), and the as-synthesised catalysts (5% w.r.t. aldehyde). The flask's contents were magnetically swirled while being heated to 343 K in an oil bath. At certain intervals, aliquots of the heated mixture were taken out to see how things were doing with the reaction. To analyse the liquid products obtained, a procedure was followed. Initially, 10 ml of diethyl ether was added to the reaction mixture, and then the mixture underwent centrifugation. The liquid products were subsequently characterized using GC.

In this study, a Clarus 680 GC instrument was employed, equipped with a merged silica column packed with Elite-5 MS (composed of 5% biphenyl and 95% dimethyl polysiloxane), measuring 30 meters in length, 0.25 millimetres in diameter, and 250 meters in film thickness. The separation of components was achieved at a constant flow rate of 1 ml/min, with helium serving as the carrier gas. To identify the products precisely, GC-MS (Gas Chromatography-Mass Spectrometry) analysis was employed, utilizing a Perkin-Elmer instrument. The mass of the products was determined using a Clarus 600 (EI) turbo mass spectrometer with an electron impact energy of 70 electron volts (70eV). The compounds in the samples were determined by comparing their spectral data to the NIST-2008 library, which has a database of spectra for all known substances.

Results and Discussion :

<u>**Characterisation of the catalyst.**</u>

X-ray diffraction is a reliable technique for probing the crystallinity of the synthesized material. Fig.1a displays the XRD pattern obtained from Mg-BTC MOF. Figure 1a and 1b display the X-ray diffraction (XRD) patterns obtained during the analysis. The diffraction lines observed at 2θ angles approximately 11.54°, 14.74°, 19.15°, 22.00°, 24.05°, 27.39°, 30.69° and 39.14 ° have been identified and associated with specific crystal planes of the Mg-BTC MOF. These planes correspond to the (111), (210), (220), (311), (320), (410), (420) and (522) crystallographic planes, respectively. The highest intensity peak is observed at 2θ 27.39°. Fig.1b represents the PXRD pattern for TiO$_2$@Mg-BTC MOF. Bragg's Diffraction peaks are observed at 2θ's 15.84°, 18.75°, 22.04°, 23.81°, 25.29°, 26.96°, 28.89°, 29.11°, 30.16°, are associated with (210), (220), (311), (320), (321), (400), (330), (331), (420) respectively are crystal planes of TiO$_2$@ Mg-BTC MOF. Additional diffraction lines were observed at 2θ angles of 15.84°, 25.29°, 26.96°, 28.89°, and 29.11° following the deposition of TiO$_2$ onto the MOF. These new diffraction lines can be attributed to the presence of specific crystal planes of rutile, which include the (210), (220), and (321) crystal planes. This observation suggests the successful growth of TiO$_2$ on the Mg-BTC MOF, leading to the appearance of these rutile-related diffraction patterns[20]. From the XRD pattern it is evident that the TiO$_2$ was fully dispersed on the MOF material and there is no structural damage even after the growth of TiO$_2$. Anatase was found to be the dominant crystalline phase in the pure TiO$_2$ sample (XRD pattern not shown), consistent with prior research[21-24]. Scherrer's equation was employed to determine the mean crystallite size (D) using X-ray line broadening (1)[25],

$$D = \frac{0.9\lambda}{\beta_{1/2}\cos\theta} \frac{0.9\lambda}{\beta_{1/2}\cos\theta} \qquad (1)$$

Where

θ - Bragg's angle

λ - wavelength of the X-ray

$\beta_{1/2}$ - angular width at the half maximum intensity

Table 1 displays the crystallographic data validated by EXPO 2014 software for the synthesised materials.

Fourier Transform infrared analysis of the synthesized materials are presented in Fig.2a represents the Mg-BTC MOF. The broad absorption band around 3000 cm^{-1} to 3200 cm^{-1} is due to AR-H stretching vibrations of the benzene tricarboxylic acid, the bands

at 1608 cm^{-1} and 1374 cm^{-1} are assigned as residue of C=O asymmetric and symmetric stretching vibrations originating from the C=O of 1,3,5 benzene tricarboxylic acid. The FT-IR of TiO$_2$@Mg-BTC MOF in Fig 2b show weak absorption band in the region 3100 cm^{-1} is due to aromatic C-H stretching vibrations originating from the 1,3,5 benzene tricarboxylic acid. The bands at 1694 cm$^{-1,}$ are assigned as residue of C=O asymmetric and symmetric stretching vibrations originating from the C=O of 1,3,5 benzene tricarboxylic acid. Additionally absorption band at 1269 and 1091 cm^{-1} can be assigned to O-C=O symmetric and asymmetric stretching vibration and C-O stretching vibrations of unreacted BTC. The bands observed from 600 to about 950 cm^{-1} have been assigned to Ti–O bonds[26, 27]. The features at 1397 cm^{-1} and 1399 cm^{-1} are associated with the bending modes of CH$_3$ and CH$_2$ groups[28] respectively. These bands can be related to ethanol or dimethyl formamide used to synthesise the MOF matrices and TiO$_2$ nanoparticles. It is shown that in TiO$_2$@Mg-BTC MOF, the absorption bands attributed to Ti–O bonds are so strong that the bands related to Mg-BTC MOF from 500 to 600 cm^{-1} are barely visible.

Surface area of the materials TiO$_2$@ Mg-BTC and Mg-BTC MOFs was found to be 375 m^2/g and 893 m^2/g respectively. Significant changes in specific surface area A$_{BET}$, pore volume Vp, and pore diameter dp occur when titanium is included in the frameworks. The decrease in surface area of the TiO$_2$@Mg-BTC MOF is due the presence of TiO$_2$ nanoparticles on the pores of the Mg-BTC frameworks. Table 2 displays the synthesised MOFs' textural characteristics. The morphologies and the microstructure of the synthesized MOF materials were investigated by scanning electron microscopy (SEM).The SEM micrograph Fig 3(a) shows distribution of particles in Mg-BTC MOF as needle like crystals. A magnification at 30μm confirm these needles as irregular rod like particles. The SEM images of TiO$_2$ @ Mg-BTC MOF Fig 3(b) shows the distribution of TiO$_2$ particles in Mg-BTC MOF. It exhibits an irregular morphology, which is similar to the shape of previously reported PSM MOFs in the literature[20].

Thermogravimetric analysis (TGA) showed that the temperature in the limits of 25-800°C increase at 10°C per minute when exposed to a N$_2$ environment. Weight loss of 15% was observed after 200°C in the TGA result of the synthesised Mg-BTC MOF (see Figure 4), which corresponds to the loss of water and ethanol molecules. At temperatures over 400°C, Mg-BTC MOF decomposed into metal oxide and lost its structural integrity. According to the results, the Mg-BTC MOF framework was highly stable at temperatures below 500°C [20,29]. While in the case of **TiO$_2$@ Mg-BTC MOF, the material shows very little weight loss of 2 to 5% throughout the heating process, from which it is obvious that there is no**

significant weight loss and the post synthetically modified material remains unchanged even at 800°C, which is probably due to TiO$_2$ doping. Thus **TiO$_2$@Mg-BTC MOF shows extra ordinary thermal stability over Mg-BTC MOF.**

Catalytic Studies of Mg-BTC and TiO$_2$ @ Mg-BTC MOFs.

The catalytic activity of the synthesised materials for cyanosilylation of aldehydes was explored by using 5 wt% of MOF w.r.t aldehydes. Specifically, the study focused on examining the catalytic potential of Mg-BTC MOF for cyanosilylation of aromatic aldehydes due to its uniformly dispersed Lewis acid sites and the porous structure present throughout its entire framework[30]. Cyanohydrin formation through the addition of cyanide to carbonyl compounds is a fundamental C-C bond-forming reaction in organic chemistry and has played a pivotal role in various chemical advancements[31, 32]. As such, the catalytic capabilities of both Mg-BTC MOF and TiO$_2$@Mg-BTC MOF were assessed for their ability to facilitate the reaction between trimethylsilyl cyanide (TMSCN) and benzaldehyde, as well as various substituted benzaldehydes.

The results, as depicted in Table 3, revealed that compared to TiO$_2$@Mg-BTC MOF, Mg-BTC MOF exhibited significantly lower catalytic activity in this reaction, resulting in a notably reduced yield. The incorporation of titanium dioxide (TiO$_2$) nanoparticles into MOF structure leads to a significant enhancement in catalytic performance. The synergetic interaction between TiO$_2$ nanoparticles and the MOF framework not only increases the active sites available for catalysis but also promotes improved mass transport and stability, rendering TiO$_2$ doped MOFs as highly effective catalyst for cyanosilylation reaction[19]. It was also observed that the presence of different substituents around the benzylic portion of the benzaldehyde backbone influenced the reaction yields, indicating the impact of electronic effects and steric hindrance. For instance, yields of 87% and 89.7% were obtained for 4-methoxybenzaldehyde and 4-hydroxybenzaldehyde, while the yield for 4-nitrobenzaldehyde reached 98%[33]. This suggests that substrates functionalized with electron-withdrawing groups are more inclined to react in this context. Schematic representation of the cyanosilylation of aldehydes is shown in scheme 1.

Reusability of the catalyst.

A catalyst recycling test was carried out at 80°C to assess the long-term durability of the synthesised catalysts in the liquid phase reaction. The filtered-out, utilised catalyst samples were washed with diethyl ether and air-dried for 24 h. After each run, the catalysts were reactivated at 80°C in air oven for two hours before being utilised again. Figure 5 displays the outcomes of para nitro benzaldehyde conversion. Other substrates also showed similar

behaviour. The yield of the product obtained demonstrates that both catalysts shows considerable reduction in their catalytic activity. However, no abrupt change was observed, which confirms that Mg-BTC MOF and TiO_2@Mg-BTC MOF are stable and efficient heterogeneous catalysts for chemical transformations.

Conclusion :

In summary, we have synthesized Mg-BTC MOF and TiO_2@Mg-BTC MOF and demonstrated that the synthesized materials are a highly potential heterogeneous catalyst for cyanosilylation of aldehydes. Under heterogeneous circumstances, the catalytic process shows great selectivity and good yields. The catalytic activity of the synthesised materials are maintained even after repeated recycling and reuse. Our work thus shows the easy and efficient method for practical synthesis of fine chemicals via catalytically active MOFs and highlights their efficiency as a heterogenous catalyst. Our future research is dedicated to exploring the impact of post-synthetic modifications on the catalytic properties of our synthesized MOF materials and assessing their potential to compete with established industrial catalysts. We aspire to uncover any unique catalytic characteristics that may arise from these modifications and offer valuable insights into the design and application of MOFs for a wide range of organic conversions. Ultimately, our work aims to contribute to the development of MOF-based catalytic systems that can provide innovative and sustainable solutions, advancing the field of catalysis and addressing industrial challenges.

Figures:
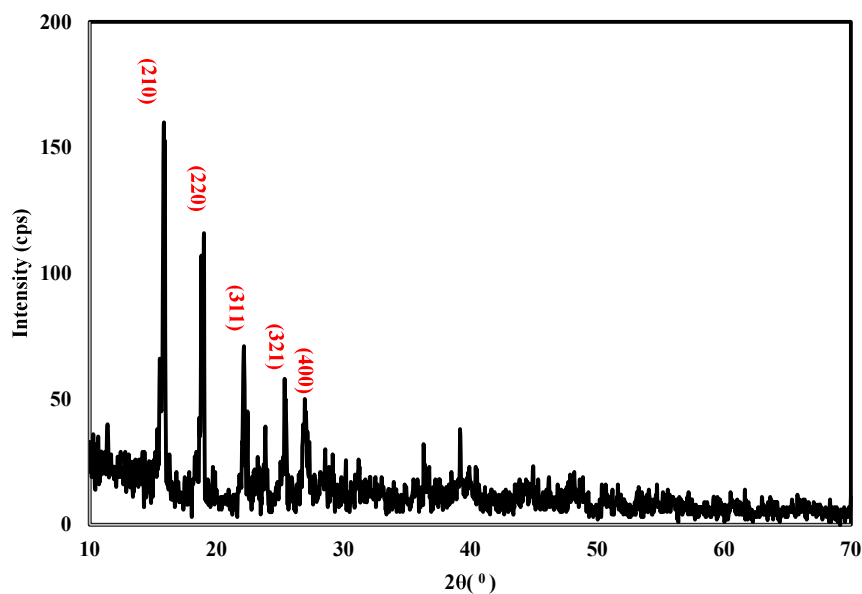
Fig. 1a PXRD image of Mg-BTC MOF.
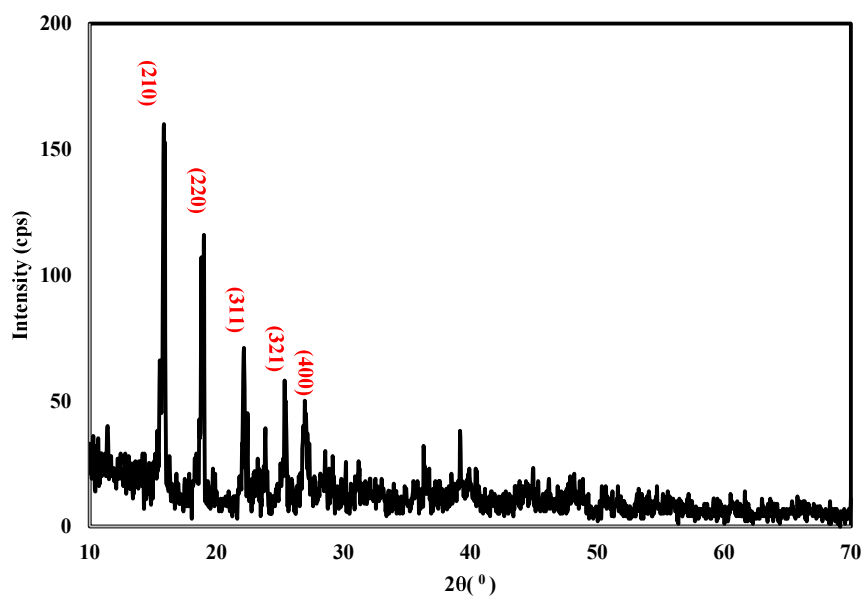
Fig. 1b PXRD image of TiO₂@ Mg-BTC MOF.
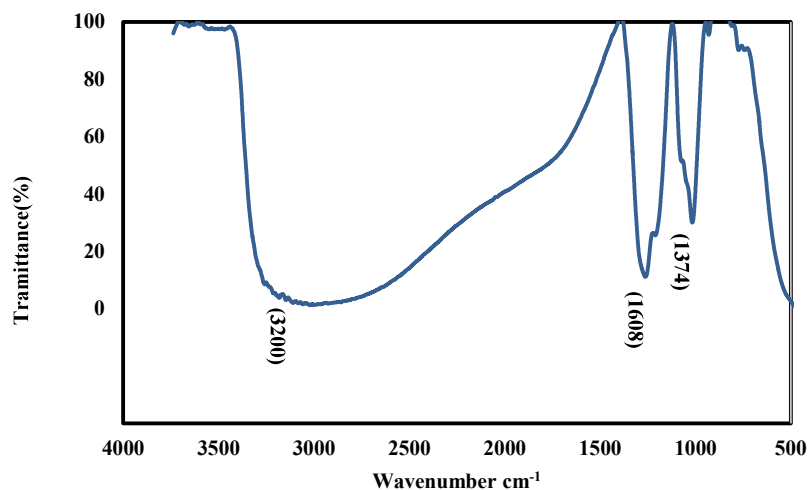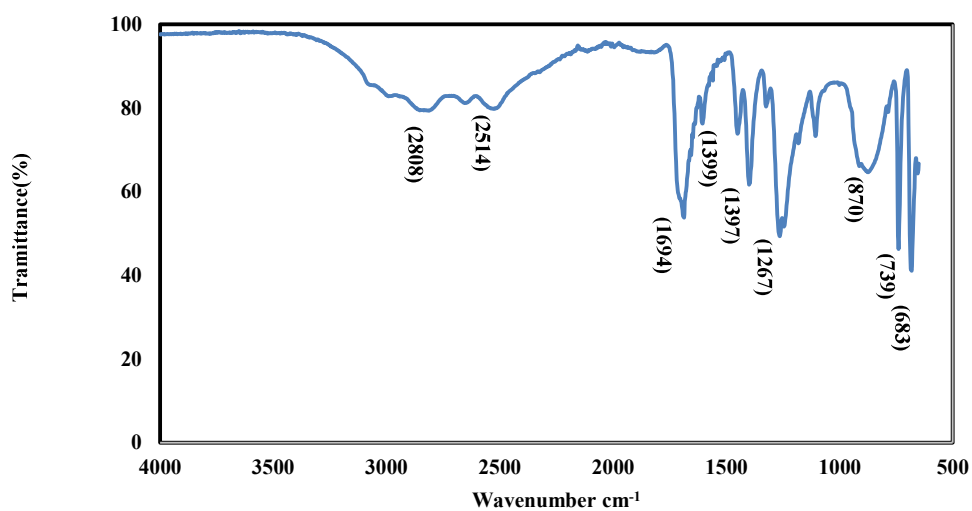
Fig. 2a FT-IR image of Mg-BTC MOF.

Fig.2b FT-IR image of TiO$_2$ @Mg-BTC MOF.

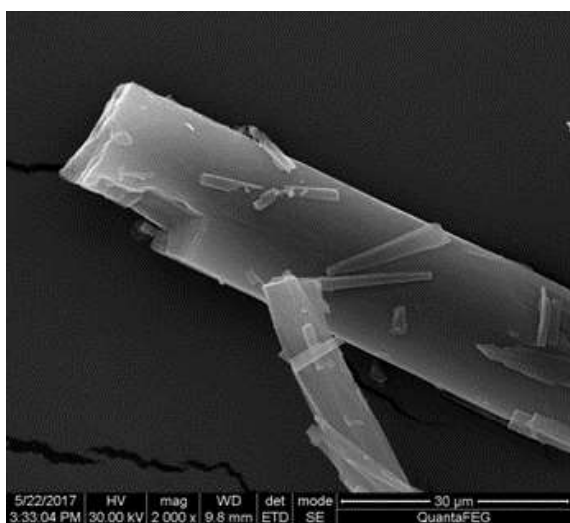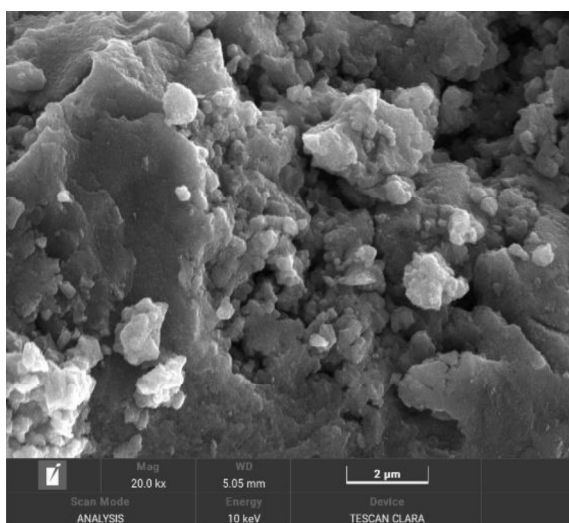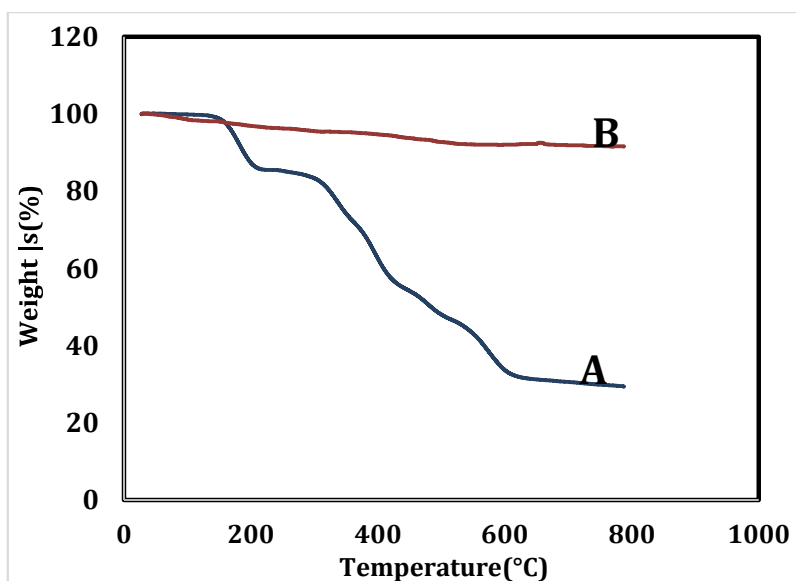**Fig. 3a SEM image of Mg-BTC MOF.**   **Fig. 3b SEM image of TiO$_2$@ Mg-BTC MOF.**

Fig. 4 Thermogravimetric analysis Spectrum of A) Mg-BTC MOF B) TiO$_2$@ Mg-BTC MOF
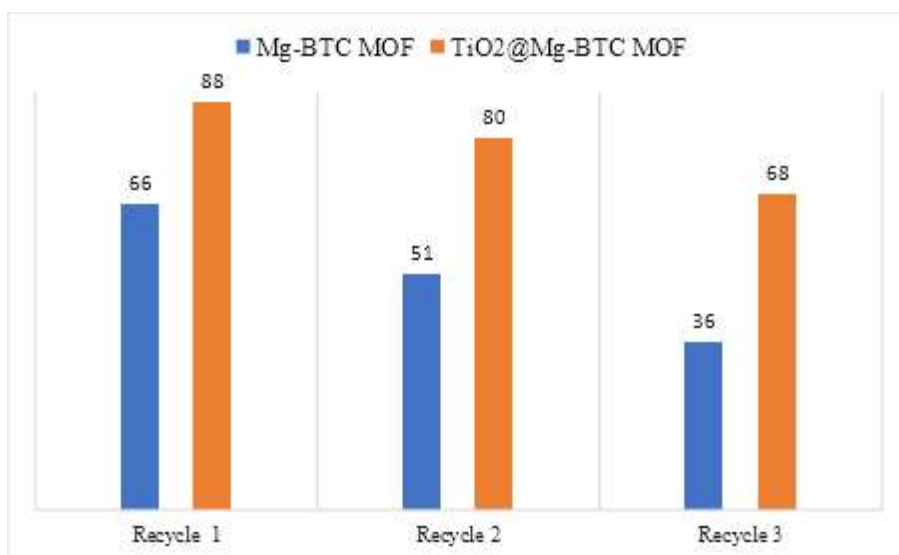

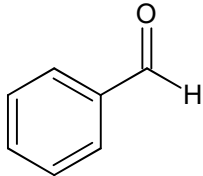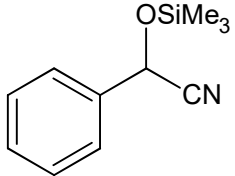**Fig.5 Reusability of Mg-BTC MOF and TiO$_2$@Mg-BTC MOF for cyanosilylation of aldehydes.**

Tables:

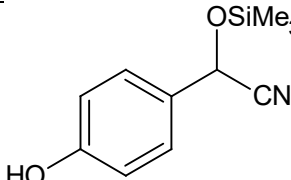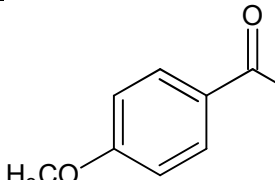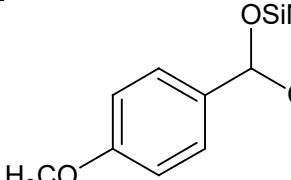**Table 1: Plausible Crystallographic data of Mg-BTC and TiO₂ @ Mg-BTC MOFs.**
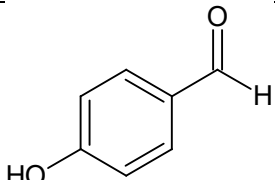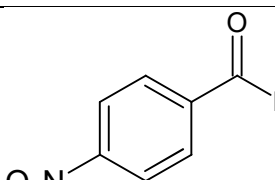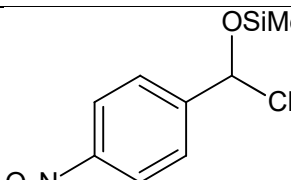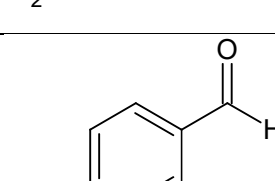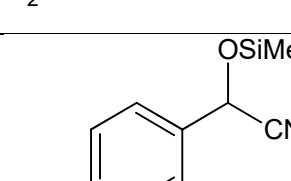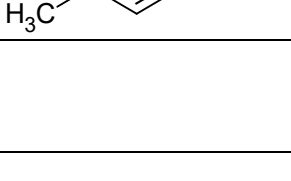
Properties	Mg-BTC MOF	TiO$_2$ @ Mg-BTC MOF
Crystal system	Triclinic	Triclinic
a [Å]	7.87097	12.38563
b [Å]	11.60119	14.61443
C [Å]	15.95049	6.20901
α [degree]	59.26130	92.52675
β [degree]	117.29031	90.24860
γ [degree]	90.33700	103.29796
V(Unit cell volume)[Å^3]	912.21	1092.57
Space group	P1	P1
D crystallite size nm	25.5614	51.62482

Table 2: Textural properties of Mg-BTC and TiO$_2$@Mg-BTC MOFs

Metal Organic Frameworks	A$_{BET}$ (m^2/g)	d$_p$ (nm)	V$_p$(cm^3/g)
TiO$_2$@ Mg-BTC	375	2.25	0.185
Mg-BTC	893	3.1	0.723

\

Table 3. Comparative study on the catalytic activity of Mg-BTC and TiO₂ @ Mg-BTC MOF

Substrate	Product	Yield %	
		Mg-BTC MOF	TiO$_2$ @ Mg-BTC MOF

		60	82.25
(4-hydroxybenzaldehyde)	(2-(4-hydroxyphenyl)-2-(trimethylsilyloxy)acetonitrile)	64	89.7
(4-methoxybenzaldehyde)	(2-(4-methoxyphenyl)-2-(trimethylsilyloxy)acetonitrile)	67	87
(4-nitrobenzaldehyde)	(2-(4-nitrophenyl)-2-(trimethylsilyloxy)acetonitrile)	75	98
(4-methylbenzaldehyde)	(2-(4-methylphenyl)-2-(trimethylsilyloxy)acetonitrile)	65	85
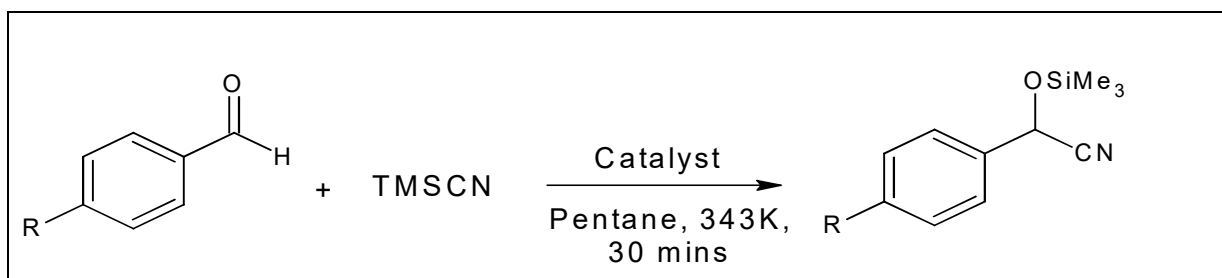
Scheme:

Scheme 1 Schematic representation of cyanosilylation of aldehydes.

References

1. J. D. Sosa, T. F. Bennett, K. J. Nelms , B. M. Liu , R. C. Tovar and Y. Liu, Crystals, 8, 325, 2018.

2. A. Aijaz, Q. Xu, J. Phys. Chem. Lett, 5, 1400, 2014.

3. K.V. Kumar, K. Preuss, M.M Titirici, F. Rodríguez-Reinoso, Chem. Rev., 117, 1796, 2017.

4. Z.R. Herm, E.D. Bloch, J.R. Long, Chem. Mater, 26, 323,2014.

5. S. Rojas, F.J. Carmona, C.R. Maldonado, P. Horcajada, T. Hidalgo, C. Serre, J.A.R. Navarro, E. Barea, Inorg. Chem., 55, 2650, 2016.

6. Y. Liu, J. Howarth Ashlee, T. Hupp Joseph, K. Farha Omar, Angew. Chem.Int.Ed., 54, 9001, 2015.

7. X.M. Li, L.Z. Dong, S.L. Li, G. Xu, J. Liu, F.M. Zhang, L.S. Lu, Y.Q. Lan, ACS Energy Lett., 2, 2313, 2017.

8. W. Huang, S. Li, X. Cao, C .Hou, Z. Zhang, J.Feng, L. Ci, P. Si, Q. Chi, ACS Sustain. Chem. Eng., 5, 5039, 2017.

9. C.T. Buru, P. Li, B.L. Mehdi, A. Dohnalkova, A.E. Platero-Prats, N.D. Browning, K.W. Chapman, J.T. Hupp, O.K. Farha, Chem. Mater., 29, 5174, 2017.

10. Z. Chen, Z.G. Gu, W.Q. Fu, F. Wang, J. Zhang, ACS Appl. Mater. Interfaces, 8, 28737, 2016.

11. H. K. Okoro, S. O. Ayika, J. C. Ngila, A. C. Tella, Applied Water Science , 8:169, 2018.

12.D. Saha, T.Maity, S. Das and S.Koner, Dalton Trans., 42, 13912, 2013.

13. J. Xu, Y. Yu, G. Li, S. Wang, Y. Liu, D. Liu and C. Wang, RSC Adv., 6 (106),104451, 2016.

14. G. Mali, J.Trebosc, C.Martineau, M. Mazaj, *J. Phys. Chem. C* , 119, 7831, 2015.

15. D. Saha, T.Maity and S.Koner**, *Dalton Trans.*, 43,** 13006, 2014.

16. S. Mandal, S. Natarajan, P. Mani, and A. Pankajakshan , Adv. Funct . Mater. 31(4), 2006291, 2020.

17. J. Rajendran, K. Tamil , D. Lokhendra, M. Preethika, A. Raji , A.Zeid , O. Mohamed and S. Ashok. Chemosphere. 287, 132106, 2021.

18. G. Sridharan, R. Atchudan, V. Magesh, S. Arya, D. Ganapathy, D. Nallaswamy, A. K. Sundramoorthy, Electroanalysis, 35, e202300093, 2023.

19. S. Chandra Kishore, S. Perumal, R. Atchudan, A.K. Sundramoorthy, M.Alagan, S. Sangaraju and Y.R. Lee, *Catalysts,* 12(12), 1501, 2022.

20.Y. Hu, Z. Huang, L. Zhou, D. Wang, G. Li, J Sep Sci, 37, 1482, 2014.

21. P. H. M. Andrade , A. L. M. Gomes , H. G. Palhares , C. Volkringer , A. Moissette , H. F. V. Victoria , N. M. A. Hatem, K. Krambrock , M. Houmard and E. H. M. Nunes,J Mater Sci , 57, 4481, 2022.

22. H. G.Palhares, B.S. Goncalves, L.M.C. Silva et al, J Sol-Gel Sci Technol, 95,119, 2020.

23. H. Hu, M. Chang, X. Wang, D. Chen, J Mater Sci , 7,55653, 2017.

24. B.S. Goncalves, H. G.Palhares, T.C.C. de Souza et al ,J Mater Res Technol, 8, 6262, 2019.

25. B.S. Goncalves , T.C.C. de Souza, V.G. de Castro et al, J Mater Res,   34, 3918, 2019.

26. A. K. Singh, S. R. Deo, G. S. Thool, R. S. Singh, Y. R. Katre And A. Gupta, J. Synth. React. Inorg. Metal-Org. Nanometal. Chem, 41(10), 1346, 2011.

27. M. Crisan , A. Braileanu, M. Raileanu et al, J Non Cryst Solids, 354,705, 2008.

28. D.C.L Vasconcelos, E.H.M. Nunes, A.C.S. Sabioni et al, J Non Cryst Solids, 07, 035 , 2012.

29. J. Yang, H. Peterlik, M. Lomoschitz, U. Schubert, J Non Cryst Solids, 356:1217, 2010.

30. J. B. DeCoste, G, W. Peterson, B. J. Schindler, K. L. Killops, M. A. Broweb and J. J. Mahle, J. Mater. Chem. A**, 1,** 11922, 2013.

31. Y. Liu, P. Zhao, C. Duan and C. He, RSC Adv., 11, 34779, 2021.

32. H. Jun, S. Oh, G. Lee and M. Oh, Scientific Reports, 12, 14735, 2022.

33.J. Du, X. Zhang, X. Zhou and D**. Li,** *Inorg. Chem. Front.***,** **5**, 2772, 2018.